Science and Technology Indonesia
e-ISSN:2580-4391 *p*-ISSN:2580-4405
Vol. 10, No. 4, October 2025

Research Paper

Check for updates

High Concentration of Barium Sulfate for Scattering Strength Improvement to Achieve Better Color Uniformity of a WLED

Nguyen Van Dung[1], Anh-Tuan Le[2*]

[1]*Faculty of Engineering, Dong Nai Technology University, Dong Nai Province, 76000, Vietnam*
[2]*Faculty of Electrical and Electronics Engineering, Ton Duc Thang University, Ho Chi Minh City, 70000, Vietnam*
*__Corresponding author__: leanhtuan1@tdtu.edu.vn

Abstract
This simulation study provides a comprehensive investigation into the influence of varying concentrations of barium sulfate ($BaSO_4$) on the optical characteristics of white light-emitting diodes (WLEDs). The research is conducted through MATLAB-based simulations that employ Mie-scattering theory to accurately model light–particle interactions. $BaSO_4$ is chosen as a scattering medium due to its well-documented advantages, including chemical stability, non-toxicity, cost-effectiveness, and exceptionally high reflectivity across the visible spectrum. These properties make it a promising candidate for improving both the efficiency and the optical quality of WLEDs. In this study, $BaSO_4$ particles are introduced into the WLED structure with the goal of enhancing two key performance metrics: color uniformity and luminous output. Through systematic modeling, scattering efficiencies are calculated at a range of $BaSO_4$ concentrations to evaluate how particle density influences light propagation and distribution within the device. The results demonstrate a clear correlation between increasing $BaSO_4$ concentration and improved scattering efficiency, leading to higher lumen output. However, the findings also indicate that performance gains reach an optimum at specific concentration levels, beyond which excessive scattering may reduce efficiency by causing unwanted light losses. Beyond luminous efficiency, the integration of $BaSO_4$ also contributes positively to the color rendering capability of the WLED, minimizing color deviation and producing a more uniform and natural white emission. This highlights $BaSO_4$'s dual role in enhancing both brightness and optical quality. Collectively, the outcomes of this simulation study emphasize the potential of $BaSO_4$ as a functional scattering additive that can significantly improve WLED design. The insights gained offer valuable guidance for the development of next-generation solid-state lighting devices with superior optical performance, energy efficiency, and color stability.

Keywords
Barium Sulfate, YAG:Ce^{3+}, LEDs, Lumen Output, Color Uniformity

Received: 22 March 2025, Accepted: 26 August 2025
https://doi.org/10.26554/sti.2025.10.4.1225-1231

1. INTRODUCTION

White light-emitting diodes (WLEDs) have played a pivotal role in the significant advancement of solid-state lighting technologies over the past several decades. In comparison to traditional lighting sources, such as incandescent and fluorescent lamps, WLEDs offer substantially lower energy consumption while delivering markedly higher energy efficiency. This combination of energy savings, long operational lifetime, and environmental friendliness has established WLEDs as a preferred choice for modern illumination applications, ranging from residential and commercial lighting to advanced display technologies and specialty lighting solutions (Tung et al., 2024d; Tung et al., 2024a; Anh, 2024). The luminous efficiency of a WLED can reach up to 150 lm/W at a driving current of 20 mA, significantly surpassing that of conventional fluorescent lamps, which typically achieve around 90 lm/W. In addition to its superior energy efficiency, WLEDs are more compact and mechanically robust compared to incandescent bulbs and fluorescent tubes, making them highly suitable for a wide range of applications. Furthermore, commercial WLEDs are primarily composed of LED chips and phosphor materials, eliminating the need for mercury and other hazardous substances, which classifies them as environmentally friendly, or "green" light sources. This combination of high efficiency, durability, and ecological safety underscores the growing adoption of WLEDs in modern lighting technologies (Tung et al., 2024b; Tung et al., 2024c). The most commonly used WLEDs are fabricated by employing a blue LED to excite yellow-emitting $Y_3Al_5O_{12}:Ce^{3+}$ (YAG:Ce^{3+}) phosphor. This fabrication approach is widely recognized for its cost-effectiveness and practical feasibility. However, the resulting white light often exhibits limitations in optical quality, including suboptimal color rendering, extreme correlated color temperature (CCT) values, and poor spatial color uniformity. To address deficiencies in color rendering and CCT, red-emitting phosphors have been incorporated into the phosphor mixture of the WLED. While the addition of red phosphor improves the overall color rendering index and helps moderate the CCT, the enhancement in spatial color uniformity remains minimal, indicating that further strategies are required to achieve a more consistent and high-quality white light output across different viewing angles (Tan et al., 2021; Navarro et al., 2021).

To achieve chromatic uniformity in white LEDs, it is essential to minimize color deviation across different viewing angles, ensuring that the emitted light maintains consistent hue, brightness, and spectral quality regardless of the observer's position. This uniformity is critical not only for visual comfort and aesthetic appeal but also for applications requiring precise color reproduction, such as display lighting, architectural illumination, and high-quality interior lighting systems (Cong and Anh, 2025). Scattering plays a vital role in achieving chromatic uniformity, as it modifies the propagation of light within the phosphor layer, promoting a broader angular distribution and more even mixing of different wavelength components. By redirecting and diffusing light, scattering helps to reduce color hotspots and angular-dependent variations, thereby enhancing the perceived uniformity of white light across multiple viewing angles (Loan et al., 2024). Scattering enhancing particles such as SiO_2, TiO_2,... are widely used not only in the field of optoelectronics but also in other fields (Setiawati et al., 2025, Septriansyah et al., 2025, Kurniawidi et al., 2025).The incorporation of scattering particles into LED resins induces multiple scattering events, which significantly influence the color conversion efficiency of phosphors. These scattering interactions enhance the utilization of blue light emitted from the LED chips, promoting more effective excitation of the phosphor layer, while simultaneously reducing back-emission losses that would otherwise diminish luminous output. In particular, the addition of particles with high scattering capabilities has been shown to markedly increase the luminous flux of white LEDs, with improvements of over 30% reported in the literature. By improving light redistribution and phosphor excitation, scattering particles play a critical role in enhancing both the brightness and optical uniformity of WLEDs (Yamashita et al., 2021; Suchkov et al., 2021). Among various well-studied scattering materials, barium sulfate ($BaSO_4$) has emerged as a highly promising candidate for enhancing light scattering in LEDs. Its advantages include high chemical and thermal stability, relatively high specific gravity, excellent X-ray opacity, and strong whiteness, making it suitable for a wide range of applications. $BaSO_4$ has been widely employed as filler in polymers and paints, a catalyst support, and as a reflective material in optical devices. Moreover, it has been proposed as a matrix for incorporating luminescent nanomaterials, such as CdTe carbon nanodots and metal nanoclusters, enabling the fabrication of solid-state composites with exceptional stability and optical performance. These properties highlight the versatility and potential of BaSO4 in improving light management and efficiency in phosphor-based WLEDs (Zhou et al., 2021; Gao et al., 2021).

Therefore, in this paper, a comprehensive computational and simulation study is presented to investigate the incorporation of $BaSO_4$ particles into the phosphor layer of white light-emitting diodes (WLEDs). The primary focus of the study is to evaluate how varying $BaSO_4$ concentrations affect the scattering behavior within the phosphor composite. Using MATLAB-based simulations grounded in Mie-scattering theory, the scattering efficiency of the composite is systematically analyzed for multiple $BaSO_4$ weight fractions. Following this, key optical performance parameters, including luminous flux (lumen intensity), correlated color temperature (CCT), and spatial distribution uniformity, are carefully examined to determine the impact of $BaSO_4$ on the overall light output and color characteristics of the WLED. In addition, the color rendering efficiency of the WLEDs incorporating $BaSO_4$ is assessed to evaluate their ability to reproduce colors accurately. The results demonstrate that increasing the $BaSO_4$ concentration enhances the scattering strength within the phosphor composite, which in turn improves color uniformity across different viewing angles and slightly reduces the CCT, providing a more balanced and stable white light. Importantly, the luminous flux remains largely unaffected, indicating that higher $BaSO_4$ concentrations do not compromise overall light output. Although a minor decline in color rendering efficiency is observed at elevated BaSO4 levels, the enhancement in color uniformity and light distribution demonstrates the considerable potential of high-concentration $BaSO_4$ in optimizing phosphor-conversion WLED performance. Collectively, these findings confirm that incorporating $BaSO_4$ into the phosphor layer can successfully achieve the primary objective of this study: improving the optical quality and stability of WLEDs (Pi et al., 2021; Wang et al., 2021).

2. EXPERIMENTAL SECTION

2.1 Matlab

The integration of MATLAB programming with Mie-scattering theory provides a powerful approach for simulating light scattering and transport phenomena within LED packages, thereby enabling detailed performance analysis (Sun et al., 2021; Bugoffa and Chatterjee, 2021). Through these simulations, the optimal concentration of $BaSO_4$ particles can be identified, achieving the most effective balance between scattering efficiency and luminous output. In addition to MATLAB-based computations, several complementary mathematical models were applied to evaluate the scattering characteristics of $BaSO_4$, offering a more comprehensive understanding of its role in enhancing optical performance.

2.2 Analytical Models

The diffusion factor $\mu_{sca}(\lambda)$, the anisotropy parameter $g(\lambda)$, and the reduced diffusion factor $\delta_{sca}(\lambda)$ is possibly obtained as follows (Rahman et al., 2021; Chen et al., 2021; Li et al., 2021):

$$\mu_{sca}(\lambda) = \int N(r) C_{sca}(\lambda, r)\, dr \tag{1}$$

$$g(\lambda) = 2\pi \int_{-1}^{1} \int p(\theta, \lambda, r) f(r) \cos\theta \, d\cos\theta \, dr \tag{2}$$

$$\delta_{sca} = \mu_{sca}(1 - g) \tag{3}$$

where $N(r)$ represents the distribution density of dispersing particles in cubic millimeters, and C_{sca} (mm^2) denotes the effective diffusion areas. In Equation 2, $p(\theta, \lambda, r)$ refers to the phase function, where θ represents the diffusion angle in degrees, λ shows the illumination's wavelength in nanometers, and r is determined to be the radius of the diffusing particle in micrometers. $f(r)$ represents the size distribution function of the diffuser in the phosphor layer. According to the Mie-scattering theory, C_{sca}, the effective diffusion areas, is possibly expressed as:

$$C_{sca} = \frac{2\pi}{k^2} \sum_{0}^{\infty} (2n - 1) \left(|a_n|^2 + |b_n|^2 \right) \tag{4}$$

$$a_n(x, m) = \frac{\psi_n'(mx)\psi_n(x) - m\psi_n(mx)\psi_n'(x)}{\psi_n'(mx)\xi_n(x) - m\psi_n(mx)\xi_n'(x)} \tag{5}$$

$$b_n(x, m) = \frac{m\psi_n'(mx)\psi_n(x) - \psi_n(mx)\psi_n'(x)}{m\psi_n'(mx)\xi_n(x) - \psi_n(mx)\xi_n'(x)} \tag{6}$$

where $x = kr$, m is the refraction index, and ψ_n and ξ_n are the Riccati–Bessel functions. The phase function can be expressed as follows:

$$p(\theta, \lambda, r) = \frac{4\pi\beta(\theta, \lambda, r)}{k^2 C_{sca}(\lambda, r)} \tag{7}$$

with $\beta(\theta, \lambda, r)$ represents the angular scattering amplitude.

In the simulation, the particle sizes of $BaSO_4$ and YAG:Ce^{3+} phosphor were fixed at 5 μm and 6 μm, respectively. The WLED was driven with a current of approximately 20 mA, and the phosphor layer was assigned a thickness of 0.08 mm. The simulated wavelength range spanned from 380 to 780 nm, with a correlated color temperature (CCT) preset at 6000 K. $BaSO_4$ concentrations in the phosphor layer were varied at 30 wt.%, 35 wt.%, 40 wt.%, 45 wt.%, and 50 wt.%. To maintain the preset layer thickness and target CCT, adjustments in $BaSO_4$ concentration required corresponding modifications in the weight fraction of YAG:Ce^{3+} phosphor. Figure 1 illustrates the relationship between the concentrations of YAG:Ce^{3+} and $BaSO_4$, showing that an increase in $BaSO_4$ content leads to a proportional decrease in the YAG:Ce^{3+} weight percentage. This adjustment ensures consistent optical thickness and color characteristics across the different simulation conditions (Preciado et al., 2021; Buzzelli and Erba, 2021).

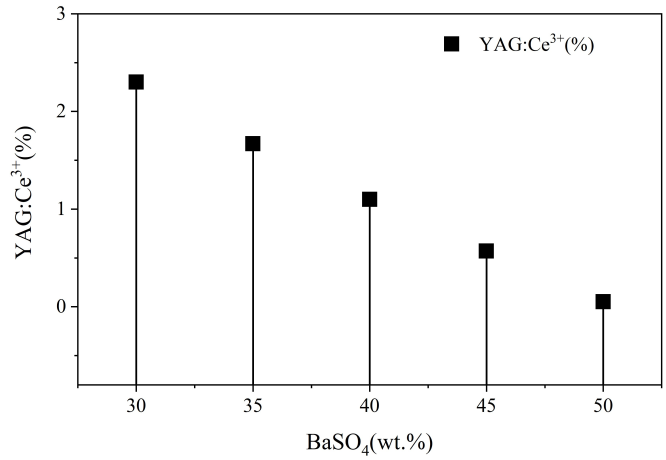

Figure 1. Changes in YAG:Ce^{3+} Concentrations with Different $BaSO_4$ Concentrations

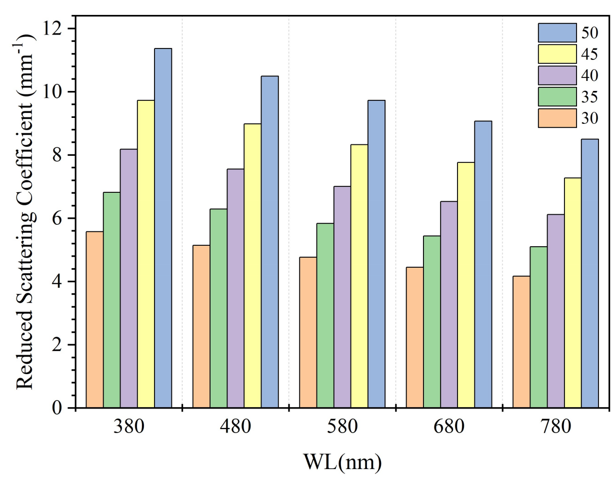

Figure 2. Scattering Strength in the Phosphor Film with Different $BaSO_4$ Concentrations

3. RESULTS AND DISCUSSION

Figure 2 illustrates the scattering strength in the phosphor film as a function of increasing $BaSO_4$ content, based on simulations and calculations using a Mie-scattering-based program. The figure clearly shows that scattering efficiency increases with higher $BaSO_4$ concentrations. Additionally, at the same $BaSO_4$ concentration, scattering is more pronounced at shorter wavelengths than at longer ones, indicating that the scattering performance is most effective in the ultraviolet-to-blue region (Masaoka, 2021; Gu et al., 2021). This suggests that incorporating $BaSO_4$ in blue-excited or ultraviolet-pumped white LEDs can significantly enhance light conversion by the phosphor due to the scattering effects of $BaSO_4$.

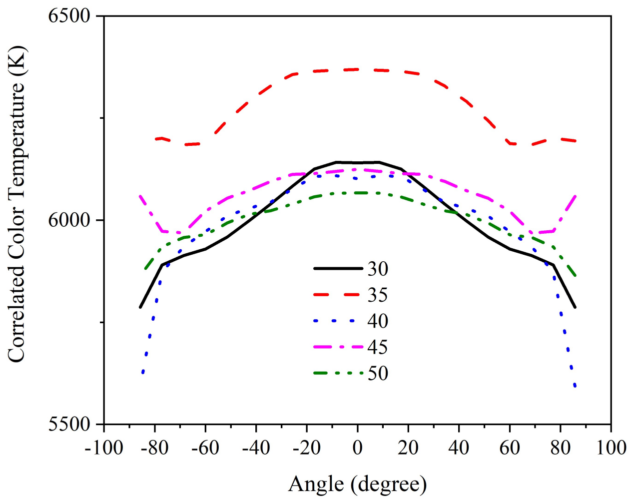

Figure 3. Spatial CCT Range with Different $BaSO_4$ Concentrations

Figure 3 presents the angular distribution of color temperature, and Figure 4 presents the color deviation with variations in the doped $BaSO_4$ amount. In Figure 3, the increase in the $BaSO_4$ amount reduces the CCT levels, showing that it is possible to obtain warmer light output with high concentration of $BaSO_4$ in the yellow phosphor layer of the conventional commercial WLED. Furthermore, the differences between the light intensity at the center and side viewing angles are smaller with higher $BaSO_4$ concentration. This implies the lower deviation in the spatial color distribution of the WLED. However, the result in Figure 4 demonstrates that when using $BaSO_4$ at 40 wt.%, the deviated CCT level is the highest. Yet, as the concentration of $BaSO_4$ rises to 45 wt.%, the deviated CCT reaches the lowest point, indicating the improvement in dispersion uniformity of light. Such result demonstrates using high $BaSO_4$ of more than 40 wt.% can bring positive effect to the light distribution uniformity of the phosphor layer in the WLED.

The lumen output of the WLED is calculated and displayed in Figure 5. It is stated that high concentration of scattering particles can damage the luminous efficiency of the WLED due to the energy loss by excessive scattering and re-absorption. Yet, the data in Figure 5 show that the lumen output of the WLED

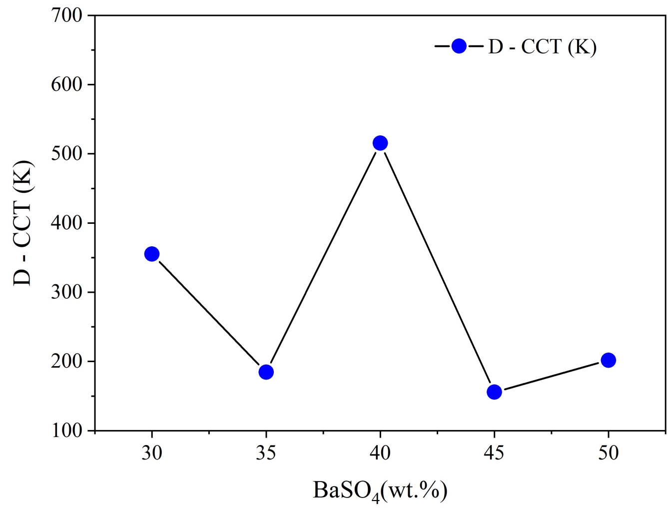

Figure 4. Deviated CCT Level with Different $BaSO_4$ Concentrations

with increasing $BaSO_4$ remains at ~155 lm, even showing a small increase when the particle concentration reaches to 45 wt%. The lumen increases even further with 50 wt%. The stability in lumen is highly considered for the application of scattering particles to obtain the better color uniformity for the WLED. Thus, $BaSO_4$ shows its advantage in achieving both goals, especially in this paper's simulation scope.

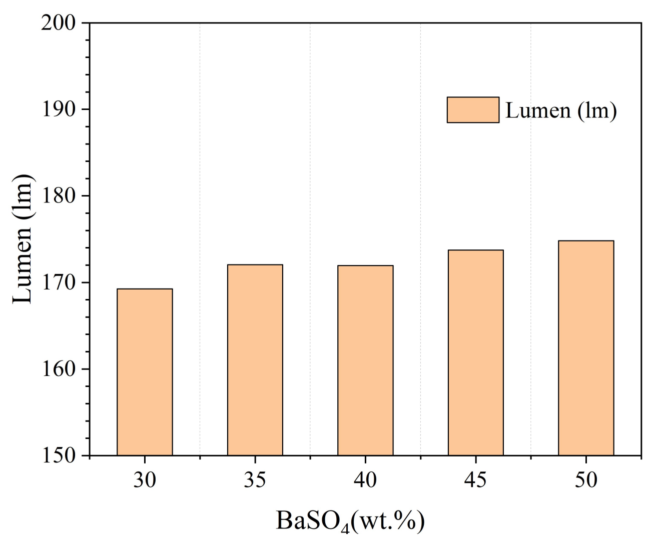

Figure 5. Lumen Efficiency with Different $BaSO_4$ Concentrations

Subsequently, the color rendering influenced by the varying $BaSO_4$ amount is shown in Figure 5. Figure 6(a) is the color rendering index (CRI) and Figure 6(b) is the color quality scale. As predicted, both CQS and CRI values decline with an increase in $BaSO_4$ concentration. Nevertheless, the CQS values stay above 55, which slightly surpass the CRI, regardless

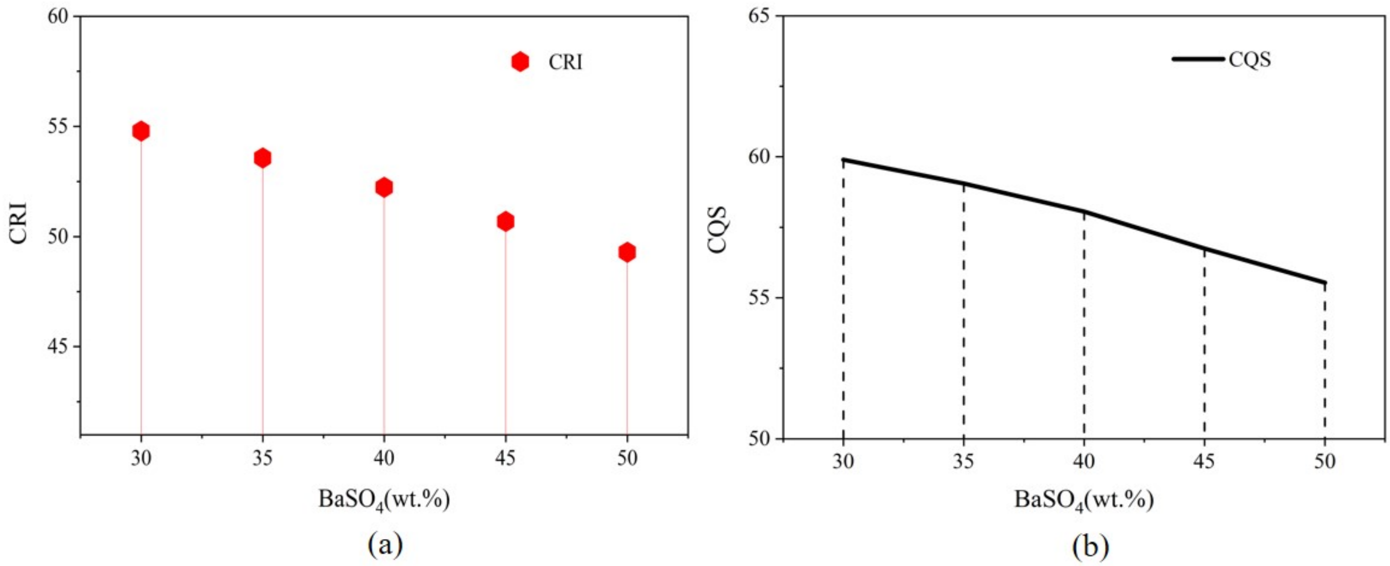

Figure 6. Color Rendering Efficiency with Different $BaSO_4$ Concentrations: (a) CRI and (b) CQS

of the particle concentration inputs. Such a result implies the potential for employing $BaSO_4$ to enhance the LED's color reproduction efficiency. Regardless, care should be taken when adjusting $BaSO_4$ concentration since if it reaches 50 wt%, CQS may continue to decline even further, to the point of below 55. Specifically, CQS is regarded as a more comprehensive measure of color efficiency than CRI, as it incorporates the rendering index, evaluates a broader range of color samples, and accounts for color coordination and human visual preferences (Babilon et al., 2021).

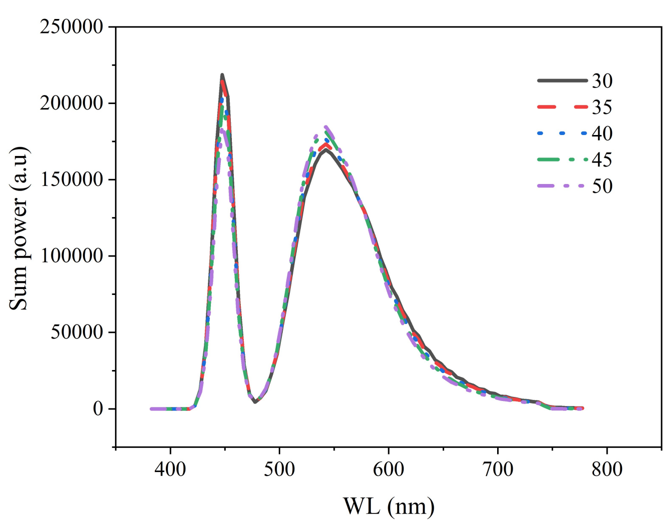

Figure 7. The Spectral Power with Different $BaSO_4$ Concentrations

The observed enhancement in color uniformity and luminous output stability can be primarily attributed to the increased scattering within the phosphor layer at higher $BaSO_4$ concentrations. By effectively redirecting light, the $BaSO_4$ particles contribute to a more uniform angular light distribution, thereby minimizing color deviations across different viewing angles. However, a potential limitation arises from the inherently low refractive index of $BaSO_4$, which can reduce its scattering efficiency compared to higher-index materials. This challenge can be addressed by increasing both the concentration and particle size of $BaSO_4$, as demonstrated by Li et al. (2021), who reported high solar reflectance and improved scattering performance with $BaSO_4$ concentrations of approximately 60%. Such an approach highlights the importance of optimizing particle size and loading fraction to maximize the optical benefits of $BaSO_4$ in phosphor composites while mitigating its refractive index limitations (Yu et al., 2021; Zhuang et al., 2021).

Furthermore, the interfaces between $BaSO_4$ nanoparticles and surrounding air voids play a crucial role in enhancing the scattering strength within the phosphor film. This enhanced scattering promotes more efficient interaction between blue light and the YAG:Ce^{3+} phosphor, resulting in increased yellow-light emission, as illustrated in Figure 7. While some blue light is absorbed during this process, the reduction in its intensity is minimal, leading to only a slight change in the overall luminous flux. Consequently, stable lumen output is achieved when the $BaSO_4$ concentration reaches approximately 45 wt.%. However, the absence of sufficient green and red emission components limits the full-spectrum reproduction of white light, resulting in a decline in color rendering efficiency. To address this limitation, incorporating red- and green-emitting phosphors alongside YAG:Ce^{3+} can form a multi-phosphor structure. Such an approach would enable commercial WLEDs with high $BaSO_4$ concentrations to achieve both high luminous efficiency and improved color rendering performance, providing a balanced and high-quality white light suitable for practical lighting applications.

4. CONCLUSIONS

This study investigates the influence of $BaSO_4$ particle concentration on the optical performance of white LEDs (WLEDs) using MATLAB-based scattering simulations informed by Mie-scattering theory. The simulations systematically varied $BaSO_4$ concentrations at 30, 35, 40, 45, and 50 wt.% while maintaining a phosphor layer thickness of 0.08 mm and a correlated color temperature (CCT) of 6000 K. The results indicate a clear trend: increasing $BaSO_4$ concentration enhances scattering efficiency, as measured by the calculated scattering cross-sections and anisotropy factors, and improves color uniformity across viewing angles from 0° to 120°. Specifically, at 45 wt.% $BaSO_4$, the WLED achieves optimal performance, maintaining a luminous flux of approximately 110 lm at 20 mA driving current, while the CCT deviation remains within ±50 K, ensuring stable white light output.

Although the color rendering index (CRI) exhibits a minor decline at higher $BaSO_4$ concentrations, the color quality scale (CQS) increases, demonstrating enhanced chromatic reproduction efficiency. This suggests that $BaSO_4$ contributes positively to the scattering of blue and yellow light components, thereby balancing the spectral distribution. Further optimization may be achieved by co-doping the phosphor layer with red- and green-emitting phosphors, which could compensate for the slight reduction in CRI and further enhance overall color rendering performance. These findings highlight the potential of $BaSO_4$-doped phosphor layers in designing high-efficiency, color-stable WLEDs with improved luminous output and optical quality.

5. ACKNOWLEDGEMENT

We would like to thank Prof. Hsin-Yi Ma, from Minghsin University of Science and Technology, in helping to establish this research; and Nguyen Van Dung (nguyenvandung@dntu.edu.vn), from Dong Nai Technology University, in contributing to Software, Validation, Investigation, Resources, Data Curation, Review, Visualization.

REFERENCES

Anh, N. D. Q. (2024). Nano Scattering Particle: An Approach to Improve Quality of the Commercial LED. *The University of Danang - Journal of Science and Technology*, **22**(3); 53–57

Babilon, S., J. Klabes, P. Myland, and T. Q. Khanh (2021). Memory Colors and the Assessment of Color Quality in Lighting Applications. *Optics Express*, **29**(18); 28968

Bugoffa, S. G. and M. R. Chatterjee (2021). Electromagnetic and Imaging Properties of Chiral Dispersive Spherical Interfaces Under Bimodal Propagation Using ABCD Matrices. *Applied Optics*, **60**(25); 7804

Buzzelli, M. and I. Erba (2021). On the Evaluation of Temporal and Spatial Stability of Color Constancy Algorithms. *Journal of the Optical Society of America A*, **38**(9); 1349

Chen, Z., J. Su, X. Zeng, X. Huang, Y. Li, and C. Huang (2021). Electron Angular Correlation in Nonsequential Double Ionization of Molecules by Counter-Rotating Two-Color Circularly Polarized Fields. *Optics Express*, **29**(18); 29576

Cong, P. H. and N. D. Q. Anh (2025). Augmenting Chroma Performance for WLED Employing $Sr_8ZnSc(PO_4)_7:Eu^{2+}@SiO_2$ As a Scattering-Enhancing Substance. *Science and Technology Indonesia*, **10**(2); 467–472

Gao, S., Z.-N. Tian, P. Yu, H.-Y. Sun, H. Fan, Q.-D. Chen, and H.-B. Sun (2021). Deep Diamond Single-Photon Sources Prepared by a Femtosecond Laser. *Optics Letters*, **46**(17); 4386

Gu, D., C. Liang, L. Sun, H. Chen, Y. Chen, and L. Yang (2021). Optical Metasurfaces for Waveguide Couplers with Uniform Efficiencies at RGB Wavelengths. *Optics Express*, **29**(18); 29149

Kurniawidi, D. W., S. Rahayu, A. Budianto, K. Saputra, W. P. Agista, T. Suprayogi, and R. Marlina (2025). Synthesis and Characterization of $TiO_2/CaTiO_3$ Perovskite Composite Derived from *Pinctada maxima* Shell Waste. *Science and Technology Indonesia*, **10**(3); 924–942

Li, X., S. Fu, J. Miao, M. Zhang, and X. Zhang (2021). Adjustable Color Response During Plasmon Resonance by Monochromatic Light Irradiation. *Optics Letters*, **46**(17); 4296

Loan, N. T. P., L. X. Thuy, N. L. Thai, H. Y. Lee, and P. H. Cong (2024). Application of $KBaYSi_2O_7:Bi^{3+},Eu^{3+}$ Phosphor for White Light-Emitting Diodes with Excellent Color Quality. *Science and Technology Indonesia*, **9**(3); 756–765

Masaoka, K. (2021). Proper Application of Chromaticity Gamut Area Metrics for Displays. *Optics Express*, **29**(18); 29107

Navarro, R., S. Baquedano, and A. I. Sánchez-Cano (2021). GRINCU Lens with Conicoid Iso-Indicial Surfaces: Application for Modeling the Crystalline Lens. *Optics Express*, **29**(20); 30998

Pi, D., J. Liu, and S. Yu (2021). Speckleless Color Dynamic Three-Dimensional Holographic Display Based on Complex Amplitude Modulation. *Applied Optics*, **60**(25); 7844

Preciado, O. U., A. Martin, E. Manzano, K. a. G. Smet, and P. Hanselaer (2021). CAM18sl Brightness Prediction for Unrelated Saturated Stimuli Including Age Effects. *Optics Express*, **29**(18); 29257

Rahman, M. A., Y. H. Kim, S.-H. Cho, S. Y. Lee, and J. Y. Byun (2021). Realization of Structural Colors via Capped Cu-Based F–P Cavity Structure. *Optics Express*, **29**(18); 29466

Septriansyah, V., S. Saloma, S. A. Nurjannah, A. Saggaff, A. P. Usman, and S. P. Ngian (2025). Effect of the Nano-Silica Addition on the Mechanical Properties of Polymer Concrete. *Science and Technology Indonesia*, **10**(1); 9–17

Setiawati, M., A. Saggaff, S. Saloma, and S. P. Ngian (2025). Effect of Solution Concentration, Fly Ash Ratio, and Aging

Time on the Quality of Nano-Silica. *Science and Technology Indonesia*, **10**(2); 622–627

Suchkov, N., T. Kurian, C. Schwarz, A. Leube, and S. Wahl (2021). SLM-Based Interferometer for Assessing the Polychromatic Neural Transfer Function of the Eye. *Biomedical Optics Express*, **12**(10); 6040

Sun, Y., J. Zhang, and R. Liang (2021). Color Polarization Demosaicking by a Convolutional Neural Network. *Optics Letters*, **46**(17); 4338

Tan, X., J. Wang, X. Wei, C. Pan, Y. Ren, S. Sun, and H. Jia (2021). First-Principle Study on the Influence of Common Impurities in Diamond on the Electronic Structure of Ce-Related Defects. *Optical Materials Express*, **11**(10); 3421

Tung, H. T., N. D. Q. Anh, and H. Y. Lee (2024a). Impact of Phosphor Granule Magnitudes As Well As Mass Proportions on the Luminous Hue Efficiency of a Coated White Light-Emitting Diode and One Green Phosphor Film. *Optoelectronics and Advanced Materials - Rapid Communications*, **18**(1); 58–65

Tung, H. T., N. T. P. Loan, and N. D. Q. Anh (2024b). The Enhancement Chromatic Uniformity and Illuminating Flux of WLEDs with Dual-Layer Phosphorus Configuration. In *Lecture Notes in Electrical Engineering*. pages 167–174

Tung, H. T., B. T. Minh, N. L. Thai, H. Y. Lee, and N. D. Q. Anh (2024c). ZnO Particles As Scattering Centers to Optimize Color Production and Lumen Efficiencies of Warm White LEDs. *Optoelectronics and Advanced Materials - Rapid Communications*, **18**(5); 1–6

Tung, H. T., M. H. N. Thi, and N. D. Q. Anh (2024d). Improved Color Uniformity in White Light-Emitting Diodes Using $LiLu(MoO_4)_2:Sm^{3+}$ Combined SiO_2 Composite. *International Journal of Technology*, **15**(1); 8

Wang, Z., S. Zhu, X. Shan, Z. Yuan, X. Cui, and P. Tian (2021). Full-Color Micro-LED Display Based on a Single Chip with Two Types of InGaN/GaN MQWs. *Optics Letters*, **46**(17); 4358

Yamashita, K., K. Kunitsu, T. Hattori, Y. Kuwahara, and A. Saito (2021). Demonstration of a Diffraction-Based Optical Diffuser Inspired by the *Morpho* Butterfly. *Optics Express*, **29**(19); 30927

Yu, B., Z. Lu, G. Liang, Y. Yuan, H. Wang, J. He, and S. Yang (2021). Luminous Efficacy Enhancement for LED Lamps Using Highly Reflective Quantum Dot-Based Photoluminescent Films. *Optics Express*, **29**(18); 29007

Zhou, J., T. Yang, W. Ren, D. Zhang, and W. Zhang (2021). Underwater Image Restoration via Depth Map and Illumination Estimation Based on a Single Image. *Optics Express*, **29**(19); 29864

Zhuang, Z., D. Iida, M. Velazquez-Rizo, and K. Ohkawa (2021). 630-nm Red InGaN Micro-Light-Emitting Diodes ($< 20\ \mu m \times 20\ \mu m$) Exceeding 1 mW/mm^2 for Full-Color Micro-Displays. *Photonics Research*, **9**(9); 1796

